NIH Public Access
Author Manuscript
J Control Release. Author manuscript; available in PMC 2011 November 20.

Published in final edited form as:
J Control Release. 2010 November 20; 148(1): 18–24. doi:10.1016/j.jconrel.2010.06.012.

Focused Ultrasound and Microbubbles for Enhanced Extravasation

M. R. Böhmer[1,*], **C. H. T. Chlon**[1], **B. I. Raju**[2], **C. T. Chin**[2], **T. Shevchenko**[3], and **A. L. Klibanov**[3]

[1]Philips Research Europe, HTC11, 5656 AE Eindhoven, the Netherlands [2]Philips Research North America, 345 Scarborough Road, Briarcliff Manor, NY105010, USA [3]Cardiovascular Division, Department of Medicine, University of Virginia, Charlottesville, VA 22908-0158, USA

Abstract

The permeability of blood vessels for albumin can be altered by using ultrasound and polymer or lipid-shelled microbubbles. The region in which the microbubbles were destroyed with focused ultrasound was quantified in gel phantoms as a function of pressure, number of cycles and type of microbubble. At 2 MPa the destruction took place in a fairly wide area for a lipid-shelled agent, while for polymer-shelled agents at this setting, distinct destruction spots with a radius of only 1 mm were obtained. When microbubbles with a thicker shell were used, the pressure above which the bubbles were destroyed shifts to higher values. *In vivo* both lipid and polymer microbubbles increased the extravasation of the albumin binding dye Evans Blue, especially in muscle leading to about 6–8% of the injected dose to extravasate per gram muscle tissue 30 minutes after start of the treatment, while no Evans Blue could be detected in muscle in the absence of microbubbles. Variation in the time between ultrasound treatment and Evans Blue injection, demonstrated that the time window for promoting extravasation is at least an hour at the settings used. In MC38 tumors, extravasation already occurred without ultrasound and only a trend towards enhancement with about a factor 2 could be established with a maximum percentage injected dose per gram of 3%. Ultrasound mediated microbubble destruction especially enhances the extravasation in the highly vascularized outer part of the MC38 tumor and adjacent muscle and would, therefore, be most useful for release of, for instance, anti-angiogenic drugs.

Keywords

microbubble; focused ultrasound; extravasation; poly-lactide; focal spot size

Introduction

Ultrasound mediated drug delivery using microbubbles, which are used in clinical practice as ultrasound contrast agents, holds promise for locally depositing a high dosage of a co-injected drug. As microbubbles stay in the vasculature, the first step in enhancing drug

© 2010 Elsevier B.V. All rights reserved.

[*]Corresponding Author: Marcel Böhmer, Biomolecular Engineering, Philips Research Europe, HTC11, 5656 AE Eindhoven, marcel.bohmer@philips.com, phone +31 40 2748252, FAX +31 40 2744906.

Publisher's Disclaimer: This is a PDF file of an unedited manuscript that has been accepted for publication. As a service to our customers we are providing this early version of the manuscript. The manuscript will undergo copyediting, typesetting, and review of the resulting proof before it is published in its final citable form. Please note that during the production process errors may be discovered which could affect the content, and all legal disclaimers that apply to the journal pertain.

NIH-PA Author Manuscript
NIH-PA Author Manuscript
NIH-PA Author Manuscript

NIH-PA Author Manuscript

NIH-PA Author Manuscript

NIH-PA Author Manuscript

delivery to non-endothelial cells is increasing the permeability of the vessel wall. In vitro work has indicated that pores or intracellular gaps are formed in endothelial monolayers and the number of these gaps depends strongly on the acoustic pressure [1,2]. Song *et al* [3] have shown that also in vivo discrete extravasation points can be identified. Increasing local extravasation has been applied to skeletal muscle [3,4], the heart [5,6], the blood brain barrier [7,8] and also to tumors [9–12]. Increasing the extravasation by ultrasound and microbubbles leads to platelet activation [13,14] showing that endothelial damage occurs *in vivo*, depending on the ultrasound settings. To obtain significant extravasation of co-administered drug, the pores should remain open for an extended time. Opening of the blood brain barrier lasts for hours [7]. Even at low pressures (0.1 MPa at a frequency of 1 MHz) Juffermans *et al* [15] have demonstrated changes in the intercellular junctions of the endothelium that already last for 30 minutes. The details also depend on the particle size or molecular weights of macromolecules chosen to probe the extravasation and on the ultrasound parameters. Extravasation can also be promoted without microbubbles but at higher pressures, Hancock *et al* [16] show that increased extravasation of nanoparticles in muscle occurs up to 48 hours after application of ultrasound.

After extravasation the mediation of cellular uptake by ultrasound is the key process to be controlled. Pore formation is the most commonly quoted mechanism to mediate cell-uptake [17–21]. The sonoporation effect mentioned by these authors lasts for seconds up to a minute. Caskey *et al* [22] show that effects of microbubbles can extend to about 7 microns beyond the endothelial wall and the jets observed [23,24] on cell monolayers would have effects beyond the monolayer as well. Transfection of cells other than endothelial cells can indeed be established experimentally as they are often very close to the endothelium as pointed out by Frenkel [10].

The phenomena outlined above depend on many parameters. From an ultrasound perspective the frequency, pressure, duty cycle and the number of cycles per pulse are the main parameters. Also different types of microbubbles can behave very differently. For instance polymer-shelled agents show little expansion and contraction on ultrasound exposure, while at not too high acoustic pressure lipid-shelled agents can show pronounced volume changes [25]. In this study we focus on the extravasation phenomenon. We compare different agents: established lipid-shelled microbubbles, which have a low destruction threshold and polymer-shelled microbubbles prepared from polylactide with a series of shell thicknesses which having a high destruction threshold. They are first compared, when incorporated in a gel, at different ultrasound settings to obtain clearly different bubble destruction patterns established by using a focused transducer. Next, these settings are applied in vivo in mice with the aim to quantify the extravasation in mouse muscle and tumor. For quantification of extravasation, an albumin binding dye, Evans Blue, was used, which can be extracted from excised tissue as reported in literature [9,26]. As many drugs bind effectively to albumin, Evans Blue is a relevant marker to study enhanced extravasation of small molecule drugs.

Materials and Methods

Agent Preparation and Characterization

Polymer-shelled microbubbles—Poly-L-lactide of a molecular weight of 2400 with a fluorinated end group was synthesized as described previously [27–28]. To prepare capsules, a 5% solution (w/w) of a polymer in dichloromethane (DCM, Merck) was prepared. To 250 mg of this solution 100, 62.5 or 37.5 mg cyclodecane (Fluka) and DCM to add up to 1 g of total solution were added. This leads to shell to core ratios of 1:8, 1:5 and 1:3. The solution was emulsified in 20 g 0.3% w/w poly-vinyl alcohol, PVA (M_w 67000, Fluka) in water, shaken to prepare a premix and then passed 10 times through an acrodisk 1 μm glass filter.

NIH-PA Author Manuscript

NIH-PA Author Manuscript

NIH-PA Author Manuscript

Subsequently, the emulsion was stirred for one hour to remove the DCM by dissolution in the aqueous phase and subsequent evaporation. After DCM evaporation the sample was centrifuged at 3000 rpm (G-force is 968g) for 30 minutes. The top fraction was retrieved and washed with 5% poly(ethyleneglycol) (PEG, Mw 3400, Aldrich) in water, after which the sample was rapidly frozen at −80°C in a pre-cooled glass vial. To remove the ice and the cyclodecane fraction, freeze-drying took place in a Christ epsilon 2–6 freeze drier for 20 hours at 1.98 mbar followed by 20 hours at 0.03 mbar. The shelf temperature of the freeze drier was maintained at −10°C. After freeze-drying the system was filled with nitrogen. Samples were stored at 4°C. Samples were redispersed to yield 10^9 microbubbles per mL. After adding saline or water, the microbubbles were put on a rotating plate for at least 15 minutes before use.

Lipid-shelled microbubbles—Microbubbles were prepared from decafluorobutane gas and stabilized with a monolayer of distearoyl phosphatidylcholine and PEG stearate [29]. An aqueous micellar dispersion of 2 mg/ml of phosphatidylcholine (Avanti Lipids, Alabaster, AL, USA), 2 mg/ml poly(ethylene glycol) stearate (Sigma, St Louis, MO, USA), was sonicated with a probe-type sonicator XL2020 (Heat Systems/Misonix, Farmingdale, NY, USA) at maximum power in an atmosphere of decafluorobutane (Flura, Newport, TN, USA). As the gas was dispersed in the aqueous phase, microbubbles were formed, which were stabilized with a self-assembled lipid/surfactant monolayer. Microbubbles were stored refrigerated in sealed vials in decafluorobutane atmosphere.

Microbubble size distributions—A Beckman Coulter (Multisizer™ 3) (Brea Ca, USA) was used to measure the particle size distribution as well as the number of particles using a 50 μm aperture tube. An aliquot is mixed with 50 ml isoton II (Beckman Coulter) from which 100 μL was analyzed in the diameter range of 1.1 μm to 30 μm.

Microbubble destruction in gels

Gel phantoms with microbubbles—Deionized water was heated up to 70°C after which 10 % (w/w) of gelatin (Bloom 4582, Roth) was added under stirring. After dissolution the solution was transferred to a 50ml Falcon tube and placed on a roller conveyor to cool down. When the solution reached 35°C, microbubbles were added. For polymer-shelled microbubbles 10^7 per mL or 10^6 per mL were introduced and for lipid-shelled microbubbles 10^6 microbubbles per mL were used. Higher concentrations for lipid-shelled microbubbles led to excessive ultrasound attenuation. Samples were allowed to cool further and the solution was poured into rectangular holders (dimensions 5.7*3.3*3 cm) just prior to reaching 30°C. and then placed in the refrigerator directly. After 60 minutes the gel was removed from the holder, submerged in a water bath and measurements were started when the gel reached room temperature.

Ultrasound Experimental Set-up for gel experiments—The gels were put in a degassed water bath on an acoustic absorber. Ultrasound was given using a Therapy and Imaging Probe System (TIPS, Philips Research, Briarcliff NY, USA), which has a focused transducer consisting of an eight element annular array [6]. The diameter and focal lengths of the transducer were both 8 cm. The transducer has an opening to hold an imaging transducer, for which a phased array, P7-4 was chosen. Imaging was performed using a HDI5000 system. Images were obtained in the B-mode with a low persistence, a frame rate of 78 Hz and an MI of 0.10, at a depth of 10 cm. More detailed images were taken after exposure using a CL15-7 probe to measure the P and S planes as indicated in Figure 1. Images were obtained in the B-mode with a depth setting of 3 cm, with persistence ‘off’ and a frame rate of 57 Hz. The MI was set at 0.16 or 0.26 for a lipid or polymer capsules filled gel respectively. For the focused ultrasound a frequency of 1.2 MHz was chosen. The

NIH-PA Author Manuscript

NIH-PA Author Manuscript

NIH-PA Author Manuscript

pressure was varied between 0 and 4 MPa and the number of cycles was varied up to 10000. Single point exposures were performed as well as a seven point pattern with a spacing of 2.25 mm between the points as shown in Figure 2. The treatment scan of 7 points was repeated 11 times for a total duration of 5 minutes unless indicated differently.

In vivo experiments

Ultrasound Imaging and Therapy

Ultrasound imaging was performed using a Sonos 7500 with a 15-6L probe at an MI of 0.2 (small parts exam, contrast mode). The transducer was mounted on the TIPS therapy probe holder with its imaging plane perpendicular to the direction of therapeutic ultrasound. The TIPS focal spot was placed about 1 mm beneath the skin. For the experiments a 1.2 MHz pulse and in most cases 2 MPa and 10000 cycles were used at each location of the therapy transducer. (See details below). The therapy transducer was moved in the same seven point pattern as for the gel experiments. The treatment scan of 7 points repeated 11 times ensured 4 seconds between pulses which allows for sufficient time for refill of the vessel with fresh microbubbles [3].

Animal protocol

All experiments were conducted in accordance with the animal guidelines of the ACUC, University of Virginia. Female C57BL/6 mice of about 30 grams were subcutaneously injected with 200,000 MC38 cells (courtesy Dr. J. Schlom, NIH) on the left leg directly after hair removal using Nair creme. Tumors developed for 10–13 days reaching a length of 7–9 mm before treatment was started. Animals were anaesthetized with isoflurane and subsequently put on a heating pad, while applying a maintenance dose of isoflurane. Ample ultrasound gel was applied around the left leg. Evans Blue, 50 μL of a 20 mg/ml solution in saline was injected retro-orbitally, followed 5 minutes later by microbubbles, $5*10^7$ in 50 μL. All injections were done slowly, in about 15 seconds, with a 28G, ½” needle. When the agent was detected to flush into the tumor, usually within 20 seconds, the ultrasound protocol was started and continued for 5 minutes. The 5 minutes of treatment time was chosen based on the observed circulation by ultrasound imaging for both types of microbubbles, which showed that for about 5 minutes microbubbles remain circulating in the major vessels in the mouse leg. Ten minutes after the first injection of microbubbles the second injection was given and the treatment repeated. Thirty five minutes after the Evans Blue injection the animals were euthanized under anaesthesia by cervical dislocation. For the experiments in which only muscle was exposed to ultrasound the injection schedule was varied to inject Evans Blue before or after ultrasound treatment the mice were euthanized, under anaesthesia, 35 minutes after Evans Blue injection. Subsequently, the skin covering the tumor was removed and photographs were taken, followed by removal of the tumor, and 2 samples of the muscle, one under the tumor and another piece of muscle tissue 2–3 mm next to the tumor.

Initial experiments were performed for an orientation on the effects of the pressure and the number of cycles, choosing 10,000 and 100 cycles at 2 MPa for the experiments on muscle. For tumor treatment, 2 MPa and 10,000 cycles were used. The animals were randomly divided over 4 groups: lipid microbubbles plus ultrasound, polymer microbubbles plus ultrasound, no microbubbles plus ultrasound and polymer microbubbles but no ultrasound (control). Polymer microbubbles were chosen for the control as they have less risk of being destroyed during imaging. All animals, also those of the control group were placed under the therapy probe and the exposure pattern was applied, but with the therapeutic ultrasound turned off for the control group. For quantification, only those animals for which no

NIH-PA Author Manuscript

NIH-PA Author Manuscript

NIH-PA Author Manuscript

remaining Evans Blue was detected under skin at injection site in the eye as indication of an injection quality were used, which led to 4 groups of 3 animals.

Evans Blue extraction

Evans Blue was extracted from tissue following a protocol adapted from that of Bekeredjian *et al* [9]. The 30–100 mg samples were freeze-dried overnight on a virtis system. Subsequently 300 μL of formamide (FMD-FX0425-3) was added. Extraction took place for a minimum of 10 hours, during which the sample was at 60°C for two hours. Absorption of Evans Blue was measured from 100 μL samples on a biorad 3550 plate reader at 595 nm. A calibration curve was prepared with Evans Blue concentrations between 3 and 60 μg/ml in formamide and, as a reference the extraction procedure was applied to tumor and muscle tissue not expose to ultrasound. All calculated amounts are expressed in percentage injected dose per gram (%ID/g) of tissue. Statistical analysis was performed with a standard t-test, unpaired, equal variance, 2-tailed distribution accepting a p-value <0.05 as statistically significant.

Results

Size distribution

The size distribution of the polymer-shelled microbubbles with a ratio shell to core 1:8 and that of lipid-shelled microbubbles is given in Figure 3A. The polymer-shelled microbubbles had a modal diameter at 1.74 μm and only a small percentage of bubbles was larger than 4 μm, the coefficient of variation was 35%. The lipid-shelled microbubbles had a slightly higher modal diameter, 2.34 μm and a similar coefficient of variation (36%). The polymer-shelled agents with thicker shells (1:5 and 1:3 ratio) had the same size distribution as the thin-shelled polymer microbubbles as shown in the Figure 3B. We have previously shown that the size distribution is not affected by free drying and that cyclodecane is removed quantitatively [27].

Destruction patterns in gels

Figure 4 shows the ultrasound images of the bubble containing gels, taken perpendicular to the direction of the focused ultrasound (indicated by line S in Figure 2 for 0.5, 1, 2, 3 and 4 MPa at 10000 cycles and 11 loops over the 7-point pattern. For the lipid-shelled agent at 0.5 MPa 7 destruction dots are visible, which merge into a large destruction zone with a diameter of 10 mm at higher pressure. For the polymer-shelled agent no destruction could be detected at 0.5 MPa and at 2 MPa a distinct dotted pattern was still obtained. Results for higher pressures showed that at 3 MPa and more the spots for the polymer-shelled agent also merged into single large destruction zones, very similar to that of the lipid bubbles at 2 MPa. Along the other axis, indicated by P in figure 5, where data are shown for exposure on one spot, a clear ellipsoid shape appears for 1:8 polymer-shelled microbubbles up to 2 MPa. At higher pressures the shape becomes more conical and bubble destruction occurs well before the focus of the transducer in a wide range. The measurements were repeated with 10^6 polymer microbubbles per mL, and no differences were found. The profiles did also not change if 100 or 1000 cycles were used compared to 10000 cycles. However, if only a single exposure on each spot is applied the destruction zones are less clear, independent of the number of cycles per pulse.

Figure 6 gives the diameter of the single destruction spot for lipid and polymer-shelled microbubbles with different shell thicknesses. A threshold > 0.5 MPa was found for all polymer-shelled microbubbles studied. Microbubbles with thicker shells were more difficult to break, in the gel and more than 1 MPa is needed for the thickest shell. For pressures up to 4 MPa the 7 points of destruction were still separately detected as presented in Figure 6

NIH-PA Author Manuscript

NIH-PA Author Manuscript

NIH-PA Author Manuscript

In vivo

Tests on stimulated extravasation in muscle were performed with polymer-shelled microbubbles on the right leg on which no tumor was implanted, see Table I. At 10000 cycles a distinct, homogeneous blue spot was found, which after extraction showed an %ID/g of 5.8%. Experiments were also performed where Evans Blue was injected after the ultrasound-microbubble treatment which also gave a blue coloration, but with a larger spot size (about 20 mm) and an ID/g of 9% after 35 minutes of Evans Blue circulation. Even if Evans Blue was injected 1 hour after finishing the treatment 4.3% ID/g was found, but in a smaller spot. If the ultrasound was restricted to 100 cycles instead of 10000 the %ID/g was about the same but the spot size decreased to 7–8 mm. In all cases a homogeneous coloration is observed and not the spotted pattern as observed in the gels at same ultrasound settings.

For the experiments on tumors the blue coloration of the tumor is not evident, often a number of blue spots are seen. This is also the case for tumors not exposed to ultrasound, where Evans Blue extravasates because of the leakiness of the tumor vasculature. A blue rim around the tumor is observed sometimes. For smaller tumors, we did observe more homogeneous coloration in previous experiments. If both lipid-shelled and polymer-shelled microbubbles are used, coloration of the muscle around the tumor was observed, where the total length of the blue spot was 11–13 mm. Results of the quantification after extraction are given in Figure 7. The extraction results show that Evans Blue is also present in tumors. Differences between the average values in tumors between the groups exist, but are not statistically significant; all *p*-values are above 0.05. Lipid-shelled microbubbles lead to an %ID/g of 3.2%. For polymer-shelled microbubbles the results were 2.2% and without microbubbles 1.4%. Injecting polymer microbubbles and imaging them at an MI of 0.2, but not giving therapeutic ultrasound, gives a %ID/g of 1.6%.

For muscle amounts detected are below the detection limit of 0.5%ID/g without ultrasound, and therefore the increase in Evans Blue concentration with polymer-shelled microbubbles and ultrasound is at least a factor 7–10. For the microbubble plus ultrasound combinations the %ID/g is about equal to that of the tumors. The extravasation in muscle between the bubbles plus ultrasound group and the control group was statistically significant.

Discussion

The size distributions of the microbubbles used in this study are similar. The lipid-shelled agent has a slightly broader size distribution and larger modal diameter than the polymer-shelled agents. We have chosen to use the same number of microbubbles for injection and therefore a larger gas volume was injected for the lipid-shelled microbubbles. As the size also affects the blood kinetics, this does not directly impose that the gas-volume in the region of interest was higher.

The lipid-shelled microbubbles have a low destruction threshold; using the 15-6L transducer of the Sonos system at a mechanical index of 0.2, bubble destruction is already detected during imaging. In a water bath, at 1 MHz a destruction threshold for the polymer-shelled microbubbles with the shell to core ratio 1:8 as used in these experiments was found to be 0.5 MPa. [27–28] The increments in pressures used in the experiments here do not allow for a quantitative comparison between microbubbles in gels and in water, but the order of magnitude of the destruction threshold is similar. Experiments in gels have the advantage that no acoustic streaming will occur and detailed ultrasound scans after exposure to therapeutic ultrasound are possible. No destruction is detected at 0.5 MPa for the 1:8 polymer bubble while at the next pressure studied, 1 MPa, a distinct destruction spot is found. Polymer-shelled microbubbles with thicker shells have, as expected, a higher

NIH-PA Author Manuscript

NIH-PA Author Manuscript

NIH-PA Author Manuscript

destruction threshold and, as a consequence, by choosing different shell thicknesses this threshold can be tuned to obtain a desired shape of the destruction region at any pressure between 1 and 4 MPa. This has potential application if the focus needs to be maintained for local delivery but a different interaction of the escaping gas with the tissue is required.

At high pressure the shape of the destruction region changes. Above 1 MPa destruction of the lipid bubbles also occurs outside the focal region of the transducer. For the 1:8 and 1:5 shell to core polymer agents this happened at ≥3 MPa and at 4 MPa respectively. The widening of the destruction zone with increasing pressure is expected, as in a wider area the microbubbles are exposed to pressure values above their destruction threshold. It is relevant to realize that not all microbubbles in the destruction zone have been destroyed at the same pressure; the pressure in the centre of a single spot is the highest. For translation to the *in vivo* situation this may have the consequence that microbubbles are destroyed but potentially endothelial permeability is created only above a certain pressure value generating strong interaction of the released gas with the vessel wall.

The results at different pulse lengths, or cycles per pulse, do not differ. We do, however find an effect of the number of loops over the pattern; if only a single exposure per spot takes place the local destruction is less complete. This can be due to the fact that the gas liberated from the microbubbles needs time to dissolve before a next ultrasound exposure is useful for destruction of more bubbles. Ultrasound scattering by the intact microbubbles themselves are, at the concentrations used, of minor importance as no effect of the concentration was found.

Also *in vivo* no strong differences in the intensity of the blue coloration was found between 100 and 10000 cycles. However, the length of the blue spot was significantly smaller for 100 cycles than for 10000 cycles. At 10000 cycles the length of the blue region in the muscle is 11–13 mm. This is larger than the destruction zone of the microbubbles in gel, especially for the polymer-shelled microbubbles. When Evans Blue was injected after the treatment even larger blue spots were found. In vivo, it was difficult to quantify bubble destruction locally due to inhomogeneity of the tissue and the limited contrast of the polymer-shelled microbubbles below the destruction limit. The ultrasound scattering by tissue and tissue interfaces may reduce the focus but the predominant mechanism is probably that albumin is able to diffuse through muscle tissue. At the long pulses given, Hancock *et al* [16] have shown that diffusion through muscles can be increased by enlarged gaps between muscle fibers as a consequence of ultrasound in the absence of microbubbles. So extravasation followed by diffusion will be a relevant contributing mechanism, specifically for muscle. The %ID/g values in the muscle on the tumor-free leg are significantly higher than on the tumor bearing leg. In the presence of the tumor the ultrasound scattering might be changed, and the focus of the transducer was aimed at the tumor, not the muscle, which can explain the observation.

Although we did not observe visual differences in coloration between 100 and 10000 cycles, we decided to do the series for the quantitative determination with 10000 cycles. This is based on the observation that in therapy settings fairly long pulses are often used as pointed out in the introduction, of which we re-iterate a number of settings here. Hwang *et al* [30] found a larger region in which vessel damage occurs at pressures of 1, 3, 6.5 and 9 MPa. In the study of Hwang *et al* hemorrhage was detected for pressures from 3 MPa onwards (1.17 MHz, 500 cycles). In other studies where ultrasound settings were optimized to maximize extravasation or gene expression Miller and Song [12] found a maximum expression of luciferase in tumors after treatment with plasmid DNA coding for luciferin in the presence of Optison exposed at 2 MPa, 200 ms pulses, 1.55 MHz. At higher pressures less gene transfer and more cell damage occurred as judged from effects on tumor growth at 6 and 8

NIH-PA Author Manuscript

NIH-PA Author Manuscript

NIH-PA Author Manuscript

MPa. When opening the blood brain barrier[31] the burst length is an important parameter; lengths of 10 ms are typically chosen. Ghanem [32], finally, also used 10000–20000 cycles to enhance the transendothelial transport of stem cells. If long times between the pulses are used, replenishment of the vessels in between pulses will be more complete [3]. The length of these pulses is much longer than needed for microbubble destruction. A potential explanation could be in the additional effect that is caused on tissue, especially muscle tissue as recently shown by Hancock *et al* [16].

Although the uptake we find in muscle is pronounced, the differences in tumor uptake are small, a factor 2.3 for lipid-shelled bubbles and 1.6 for polymer-shelled microbubbles (p-values 0.1). This is smaller than the difference found by Bekeredjian *et al*, who found a factor of 5 for hepatomas in rats. Yuh *et al* [33] found a factor of 2 for the uptake of doxorubicin at higher pressures but without microbubbles in SCC7 tumors. Tumor data depend to a significant extent on the natural extravasation in the specific tumor and are subject to large variations in the tumor structures with highly vascularized regions next to a necrotic core. We did not notice any blue coloration of the necrotic part of the tumors. So enhancement, if occurring ($p = 0.1$) takes place in the highly vascularized region of the tumor. For larger tumors this was often visible as a blue rim around the tumor. Bekeredjian *et al*[9] found no significant extravasation in muscle under the tumor. They also did not find increased extravasation if Evans Blue is given after ultrasound treatment, which is contrary to findings by Seip *et al*[6] (myocardium), Hancock *et al*[16] (muscle) and Yuh *et al*[33] for dextran-fluorescein in tumors. In the three latter studies long pulses of 10 ms or more were used. Pulse length is therefore a key parameter in future study of ultrasound triggered drug delivery. Deposition of drug not only in, but also around the tumor can be beneficial for cancer treatment; signalling to form for instance new blood vessels is a process occurring outside the tumor and anti-angiogenic drugs would best perform in this region.

The differences between lipid-shelled and polymer-shelled microbubbles are small even though they have significantly different destruction zones in gels. This can be related to the possibility that not all destroyed bubbles contribute to the increase in the permeability of the vasculature but also to, for instance, diffusion effects occurring after opening the endothelium, masking potential differences.

The experiments directly on the muscle indicate that the openings that are formed in the endothelium remain open for at least one hour and a high percentage injected dose per gram can be reached. Injecting Evans Blue after the treatment even gave somewhat higher percentages. This is likely because Evans Blue is injected after making the pores, while in the case of injecting Evans Blue before, the pores still need to be made and the number increases over the time of treatment (here we have also allowed 35 minutes between Evans Blue injection and euthanasia). As extravasation is still observed it seems that very high dosages, possibly 20%ID/g, can be reached in a mouse with this method when long circulating hydrophobic small molecule drugs can be used. The pores are resealed with a wound-healing mechanism, as shown by platelet activation [13,14] and increased leukocyte activity [34]. This underlines the important differences between extravasation and cell-uptake, for which the cells have to stay alive, while for extravasation some cell death and an inflammatory reaction can help to make the extravasation step efficient.

With a range of polymer microbubbles and lipid microbubbles clearly different destruction zones can be established in gel phantoms, allowing for control of destruction with a highly focused transducer to a small spot at high pressures. This does not translate into clear differences in extravasation of Evans Blue *in vivo* in tumors and muscle in the model studies. In MC38 tumors, the natural extravasation is significant and heterogeneous. This makes it difficult to quantify the enhancement and we can only observe a trend to an

NIH-PA Author Manuscript

NIH-PA Author Manuscript

NIH-PA Author Manuscript

increase with about a factor 2. In muscle, at the long pulses used, high percentages injected dose per gram tissue can be reached, especially because extravasation continues for at least an hour after ultrasound and microbubble treatment and an additional contribution of ultrasound on the diffusion through muscle is present.

Acknowledgments

We thank Dr. J. Schlom (NIH) for making MC38 cells available for this study and Martijn Dingemans for optimizing the gel phantom preparation protocols.

This research is funded by NMP-LA-2008-213706 Sonodrugs (MB and CC) and NIH R33CA102880 (AK, TS and CCC).

References

1. Nixdorff U, Schmidt A, Morant T, Stilianakis TN, Voigt JU, Flachskampf FA, Daniel WG, Garlichs CD. Dose-dependent disintegration of human endothelial monolayers by contrast echocardiography. Life Sciences. 2005; 77:1493–1501. [PubMed: 15935397]
2. Stieger SM, Caskey CF, Adamson RH, Qin SP, Curry FRE, Wisner ER, Ferrara KW. Enhancement of vascular permeability with low-frequency contrast-enhanced ultrasound in the chorioallantoic membrane model. Radiology. 2007; 243:112–121. [PubMed: 17392250]
3. Song J, Chappell JC, Qi M, VanGieson EJ, Kaul S, Price RJ. Influence of injection site, microvascular pressure and ultrasound variables on microbubble-mediated delivery of microspheres to muscle. Journal of the American College of Cardiology. 2002; 39:726–731. [PubMed: 11849875]
4. Price RJ, Skyba DM, Kaul S, Skalak TC. Delivery of colloidal particles and red blood cells to tissue through microvessel ruptures created by targeted microbubble destruction with ultrasound. Circulation. 1998; 98:1264–1267. [PubMed: 9751673]
5. Geis NA, Mayer CR, Kroll RD, Hardt SE, Katus HA, Bekeredjian R. Spatial distribution of ultrasound targeted microbubble destruction increases cardiac transgene expression but not capillary permeability. Ultrasound Med Biol. 2009; 35:1119–1126. [PubMed: 19427103]
6. Seip R, Chin CT, Raju BI, Ghanem A, Tiemann K. Targeted ultrasound mediated delivery of nanoparticles: on the development of a new HIFU basedimaging device. IEEE Trans. Biomed. Eng. 2010; 57:61–70. [PubMed: 19695986]
7. Hynynen K. Ultrasound for drug and gene delivery to the brain. Advanced Drug Delivery Reviews. 2008; 60:1209–1217. [PubMed: 18486271]
8. Treat LH, McDannold N, Vykhodtseva N, Zhang YZ, Tam K, Hynynen K. Targeted delivery of doxorubicin to the rat brain at therapeutic levels using MRI-guided focused ultrasound. International Journal of Cancer. 2007; 121:901–907.
9. Bekeredjian R, Kroll RD, Fein E, Tinkov S, Coester C, Winter G, Katus HA, Kulaksiz H. Ultrasound targeted microbubble destruction increases capillary permeability in hepatomas. Ultrasound in Med. Biol. 2007; 33:1592–1598. [PubMed: 17618040]
10. Frenkel V. Ultrasound mediated delivery of drugs and genes to solid tumors. Advanced Drug Delivery Reviews. 2008; 60:1193–1208. [PubMed: 18474406]
11. Hauff P, Seemann S, Reszka R, Schultze-Mosgau M, Reinhardt M, Buzasi T, Plath T, Rosewicz S, Schirner M. Evaluation of gas-filled microparticles and sonoporation as gene delivery system: feasibility study in rodent tumor models. Radiology. 2005; 236:572–578. [PubMed: 16040915]
12. Miller DL, Song JM. Tumor growth reduction and DNA transfer by cavitation-enhanced high-intensity focused ultrasound in vivo. Ultrasound in Med. Biol. 2003; 29:887–893. [PubMed: 12837504]
13. Hwang JH, Brayman AA, Reidy MA, Matula TJ, Kimmey MB, Crum LA. Vascular effects induced by combined 1-MHz ultrasound and microbubble contrast agent treatments in vivo. Ultrasound Med Biol. 2005; 31:553–564. [PubMed: 15831334]
14. Imada T, Tatsumi T, Mori Y, Nishiue T, Yoshida M, Masaki H, Okigaki M, Kojima H, Nozawa Y, Nishiwaki Y, Nitta N, Iwasaka T, Matsubara H. Targeted delivery of bone marrow mononuclear

NIH-PA Author Manuscript

NIH-PA Author Manuscript

NIH-PA Author Manuscript

cells by ultrasound destruction of microbubbles induces both angiogenesis and arteriogenesis response. Arteriosclerosis Thrombosis and Vascular Biology. 2005; 25:2128–2134.

15. Juffermans LJM, Kamp O, Dijkmans PA, Visser CA, Musters RJP. Low-intensity ultrasound-exposed microbubbles provoke local hyperpolarization of the cell membrane via activation of BKCa channels. Ultrasound Med. and Biol. 2008; 34:502–508. [PubMed: 17993242]
16. Hancock HA, Smith LH, Cuesta J, Durrani AK, Angstadt M, Palmeri ML, Kimmel E, Frenkel V. Investigations into pulsed high-intensity focused ultrasound-enhanced delivery: preliminary evidence for a novel mechanism. Ultrasound Med Biol. 2009; 35:1722–1736. [PubMed: 19616368]
17. Karshafian R, Bevan PD, Williams R, Samac S, Burns PN. Sonoporation by ultrasound-activated microbubble contrast agents: effect of acoustic exposure parameters on cell membrane permeability and cell viability. Ultrasound Med Biol. 2009; 35:847–860. [PubMed: 19110370]
18. Kumon RE, Aehle M, Sabens D, Parikh P, Han YW, Kourennyi D, Deng CX. Spatiotemporal effects of sonoporation measured by realtime calcium imaging. Ultrasound Med Biol. 2009; 35:494–506. [PubMed: 19010589]
19. Mehier-Humbert S, Yan F, Frinking P, Schneider M, Guy RH, Bettinger T. Ultrasound-mediated gene delivery: influence of contrast agent on transfection. Bioconjug Chem. 2007; 18:652–662. [PubMed: 17419583]
20. Zhou Y, Kumon RE, Cui J, Deng CX. The size of sonoporation pores on the cell membrane. Ultrasound Med Biol. 2009; 35:1756–1760. [PubMed: 19647924]
21. Newman CM, Bettinger T. Gene therapy progress and prospects: ultrasound for gene transfer. Gene Ther. 2007; 24:465–475. [PubMed: 17339881]
22. Caskey CF, Qin S, Dayton PA, Ferrara KW. Microbubble tunneling in gel phantoms. J Acoust Soc Am. 2009; 125:EL183–EL189. [PubMed: 19425620]
23. Prentice P, Cuschierp A, Dholakia K, Prausnitz M, Campbell P. Membrane disruption by optically controlled microbubble cavitation. Nature Physics. 2005; 1:107–110.
24. Ohl CD, Arora M, Ikink R, de Jong N, Versluis M, Delius M, Lohse D. Sonoporation from jetting cavitation bubbles. Biophysical Journal. 2006; 91:4285–4295. [PubMed: 16950843]
25. Bloch SH, Wan M, Dayton PA, Ferrara KW. Optical observation of lipid- and polymer-shelled ultrasound microbubble contrast agents. Applied Physics Letters. 2004; 84:631–633.
26. Miller DL, Driscoll EM, Dou C, Armstrong WF, Lucchesi BR. Microvascular permeabilization and cardiomyocyte injury provoked by myocardial contrast echocardiography in a canine model. J Am Coll Cardiol. 2006; 47:1464–1468. [PubMed: 16580537]
27. Chlon C, Guedon C, Verhaagen B, Shi WT, Hall CS, Lub J, Böhmer MR. Effect of Molecular Weight, Crystallinity, and Hydrophobicity on the Acoustic Activation of Polymer-Shelled Ultrasound Contrast Agents. Biomacromolecules. 2009; 10:1025–1031. [PubMed: 19351154]
28. Kooiman K, Böhmer MR, Emmer M, Vos HJ, Chlon C, Shi WT, Hall CS, de Winter S, Schroen K, Versluis M, de Jong N, van Wamel A. Oil-filled polymer microcapsules for ultrasound-mediated delivery of lipophilic drugs. Journal of Controlled Release. 2009; 133:109–118. [PubMed: 18951931]
29. Klibanov AL. Microbubble contrast agents: targeted ultrasound imaging and ultrasound-assisted drug-delivery applications. Invest Radiol. 2006; 41:354–362. [PubMed: 16481920]
30. Hwang JH, Tu J, Brayman AA, Matula TJ, Crum LA. Correlation between inertial cavitation dose and endothelial cell damage in vivo. Ultrasound Med Biol. 2006; 32:1611–1619. [PubMed: 17045882]
31. McDannold N, Vykhodtseva N, Hynynen K. Effects of acoustic parameters and ultrasound contrast agent dose on focused-ultrasound induced blood-brain barrier disruption. Ultrasound Med Biol. 2008; 34:930–937. [PubMed: 18294757]
32. Ghanem A, Steingen C, Brenig F, Funcke F, Bai ZY, Hall CS, Chin CT, Nickenig G, Bloch W, Tiemann K. Focused ultrasound-induced stimulation of microbubbles augments site-targeted engraftment of mesenchymal stem cells after acute myocardial infarction. Journal of Molecular and Cellular Cardiology. 2009; 47:411–418. [PubMed: 19540842]

NIH-PA Author Manuscript

NIH-PA Author Manuscript

NIH-PA Author Manuscript

33. Yuh EL, Shulman SG, Mehta SA, Xie JW, Chen LL, Frenkel V, Bednarski MD, Li KCP. Delivery of systemic chemotherapeutic agent to tumors by using focused ultrasound: Study in a murine model. Radiology. 2005; 234:431–437. [PubMed: 15671000]

34. Chin CT, Shevchenko T, Raju BI, Klibanov AL. Control and reversal of tumor growth by ultrasound activated microbubbles. Proceedings of the IEEE Ultrasonics symposium. 2009:77–80.

NIH-PA Author Manuscript
NIH-PA Author Manuscript
NIH-PA Author Manuscript

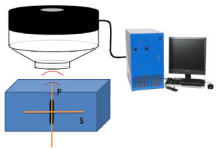

Figure 1.
Schematic overview of the therapy and imaging probe system with the microubble containing gel positioned under the transducer. The therapeutic transducer (in black) is generating focused ultrasound, driven by the control unit. In the opening of the therapy transducer (light grey) an imaging transducer can be placed. In the gel block the measurement direction is indicated, parallel (P-plane) and perpendicular (S-plane) to the focused ultrasound beam (TIPS).

NIH-PA Author Manuscript
NIH-PA Author Manuscript
NIH-PA Author Manuscript

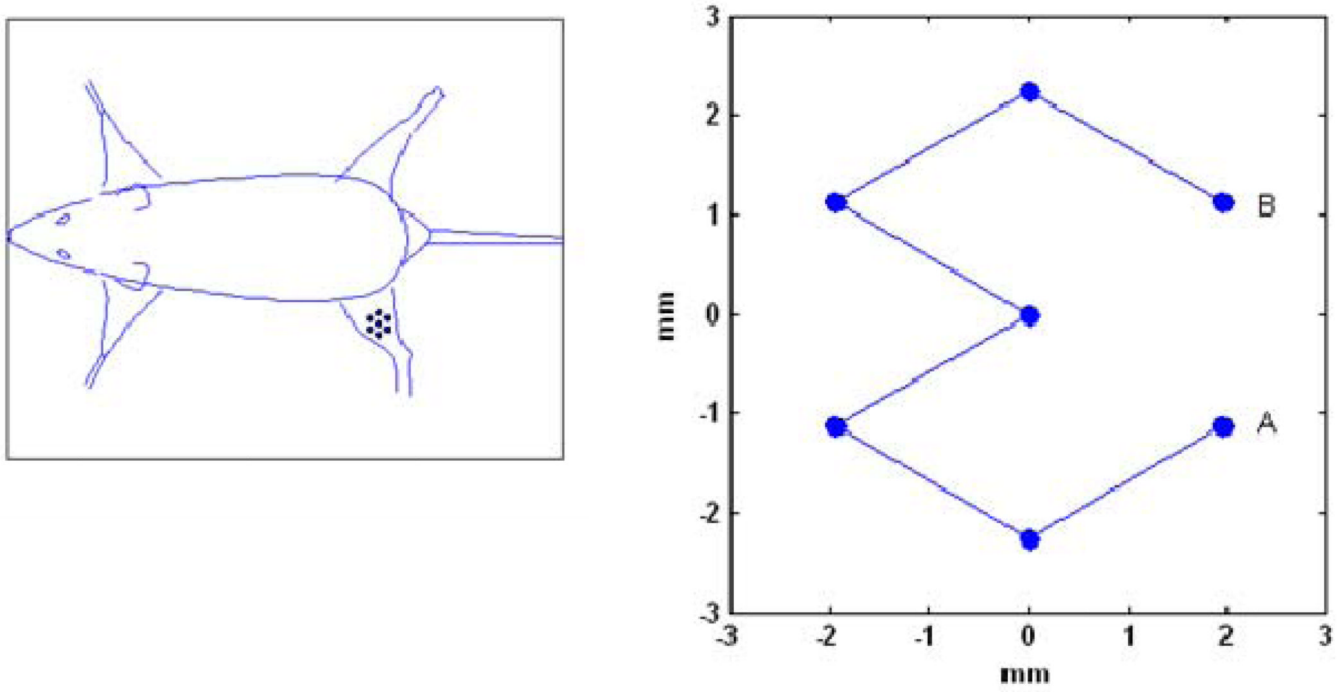

Figure 2.
seven point ultrasound scan pattern used in gels and on the mouse leg.

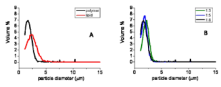

Figure 3.
size distribution of microbubbles: lipid-shelled and polymer-shelled with a 1:8 shell to core ratio (A) and polymer microbubbles with 3 different shell to core ratio's.

NIH-PA Author Manuscript
NIH-PA Author Manuscript
NIH-PA Author Manuscript

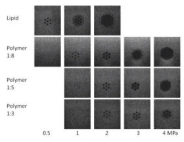

Figure 4.
Destruction pattern in microbubble containing gels after 7 point exposures, 10000 cycles, 11 loops, 1.2 MHz at 0.5, 1, 2, 3, 4 MPa for lipid-shelled microbubbles and polymer-shelled microbubbles with three shell to core ratios.

NIH-PA Author Manuscript
NIH-PA Author Manuscript
NIH-PA Author Manuscript

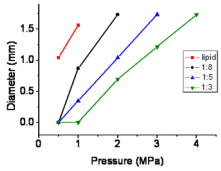

Figure 5.
diameter of destruction spots as a function of the applied pressure for lipid-shelled microbubbles and polymer-shelled microbubbles with three different shell to core ratios.

NIH-PA Author Manuscript
NIH-PA Author Manuscript
NIH-PA Author Manuscript

NIH-PA Author Manuscript
NIH-PA Author Manuscript
NIH-PA Author Manuscript

Figure 6.

destruction patterns in gels of polymer-shelled microbubbles, 10000 cycle prf 10, 2 seconds exposure at 1, 2, 3 and 4 MPa, View in the direction of the transducer (P-plane), see figure 1.

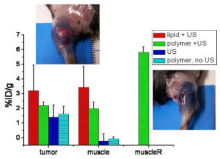

Figure 7.

% ID/g of Evans Blue in tumor, muscle around the tumor for lipid-shelled and polymer-shelled microbubbles with ultrasound, ultrasound without microbubbles and polymer microbubbles without ultrasound. MuscleR indicates the muscle on the right leg on which no tumor was grown, which was exposed to ultrasound and polymer microbubbles. Average of three experiments. The pictures give an impression of the blue coloration around the tumor and in the muscle for polymer-shelled microbubbles. Ultrasound settings: 1.2 MHz, 10000 cycle, 2 MPa, 11 loops.

NIH-PA Author Manuscript
NIH-PA Author Manuscript
NIH-PA Author Manuscript

NIH-PA Author Manuscript

NIH-PA Author Manuscript

NIH-PA Author Manuscript

Table I

%ID/g and estimation of the length of the blue spot for muscle at 10000 and 100 cycles, 7 point pattern, 1.2 MHz, 2 MPa for polymer-shelled microbubbles. Injection of Evans Blue before ultrasound, directly after ultrasound and in case of 10000 cycles also one hour after the ultrasound treatment. Averages of three animals.

EBlue injection	10000; %ID/g	10000; spot size (mm)	100; % ID/g	100; spot size (mm)
Before US	5.8 ± 0.4	11–13	8.7 ± 0.6	6–9
After US	9.1 ± 0.7	18–20	11.5 ± 4.2	6–9
60 min. after US	4.3 ± 1.9	8–10		